Neuron
Article

EphA4 Signaling in Juveniles Establishes Topographic Specificity of Structural Plasticity in the Hippocampus

Ivan Galimberti,[1,2,3] Ewa Bednarek,[1,2] Flavio Donato,[1] and Pico Caroni[1,*]
[1]Friedrich Miescher Institut, Maulbeerstrasse 66, CH-4058 Basel, Switzerland
[2]These authors contributed equally to this work
[3]Present address: Novartis Institutes for Biomedical Research, CH-4058 Basel, Switzerland
*Correspondence: caroni@fmi.ch
DOI 10.1016/j.neuron.2010.02.016

SUMMARY

The formation and loss of synapses is involved in learning and memory. Distinct subpopulations of permanent and plastic synapses coexist in the adult brain, but the principles and mechanisms underlying the establishment of these distinctions remain unclear. Here we show that in the hippocampus, terminal arborizations (TAs) with high plasticity properties are specified at juvenile stages, and account for most synapse turnover of adult mossy fibers. Out of 9-12 giant terminals along CA3, distinct subpopulations of granule neurons revealed by mouse reporter lines exhibit 0, 1, or >2 TAs. TA specification involves a topographic rule based on cell body position and EphA4 signaling. Upon disruption of EphA4 signaling or PSA-NCAM in juvenile circuits, single-TA mossy fibers establish >2 TAs, suggesting that intra-axonal competition influences plasticity site selection. Therefore, plastic synapse specification in juveniles defines sites of synaptic remodeling in the adult, and hippocampal circuit plasticity follows unexpected topographic principles.

INTRODUCTION

Structural plasticity in the intact adult nervous system includes the formation of new synapses and the loss of existing synapses. This synapse turnover could have major roles in learning and memory, but the mechanisms underlying its regulation and specificity in the adult are poorly understood (Chklovskii et al., 2004; Alvarez and Sabatini, 2007; De Roo et al., 2008a). Time-lapse imaging studies of synapses in adult mouse and monkey brains have provided evidence for the existence of distinct subpopulations of stable and dynamic synapses (Holtmaat et al., 2006; Stettler et al., 2006; De Paola et al., 2006; Gogolla et al., 2007). Stable presynaptic boutons or postsynaptic spines appear to persist indefinitely in the adult, and represent the largest fractions of total synapses (85%–92%). By contrast, dynamic synapses turn over within days or weeks in vivo. In spite of their obvious relevance to the understanding of plasticity in the adult, the mechanisms underlying the distinctions between stable and dynamic synapses are currently unknown. In particular, it is not clear whether stable synapses, dynamic synapses, or both are specified, when and how specification occurs, whether the process involves experience, and whether anatomical specificity may also be involved.

Hippocampal mossy fibers, which are the axons of dentate gyrus (DG) granule cells (GCs), are uniquely well suited models in which to investigate distinctions between stable and dynamic synapses in the adult (Henze et al., 2000). These glutamatergic axons have local target regions in the DG, and then project to CA3, where they contact principal pyramidal neurons and inhibitory interneurons (Claiborne et al., 1986; Acsády et al., 1998; McBain, 2008). Four features of the projections in CA3 are particularly important in the context of this study (Figure 1A). First, mossy fibers do not collateralize in CA3. Second, with the exception of their distal terminations in CA3a, where they extend caudally along the anterior-posterior axis of the hippocampus, mossy fibers extend in a lamellar fashion along the proximodistal axis of CA3 (Henze et al., 2000). Third, their large synaptic boutons onto pyramidal neurons in CA3 (large mossy fiber terminals, or LMTs) are few in number (8–11 per mossy fiber in the mouse), easily identifiable morphologically, and unusually potent (Henze et al., 2002; Mori et al., 2004; Rollenhagen et al., 2007). Fourth, some LMTs establish local "satellite LMTs" onto pyramidal neurons, through processes emanating from those "core LMTs" (Figure 1A) (Galimberti et al., 2006). Satellite LMT frequencies are influenced by experience in the adult, suggesting that they include dynamic synapses (Galimberti et al., 2006; Gogolla et al., 2009). As a consequence of this unique anatomical arrangement, all LMTs of individual mossy fibers along CA3 can be imaged on appropriate hippocampal sections, thus allowing the analysis of complete populations of identified presynaptic terminals by a given axon within one of its target regions. The sparse coding, low connectivity, and high potency of LMT synapses onto pyramidal neurons in CA3 imply that any rearrangement of these synapses will likely have an impact on the ensemble of CA3 pyramidal neurons recruited by mossy fibers in response to a particular behavioral context (Henze et al., 2002; Mori et al., 2004; Leutgeb et al., 2007).

Hippocampal mossy fiber terminals exhibit substantial structural plasticity in the adult. Hippocampus-dependent learning

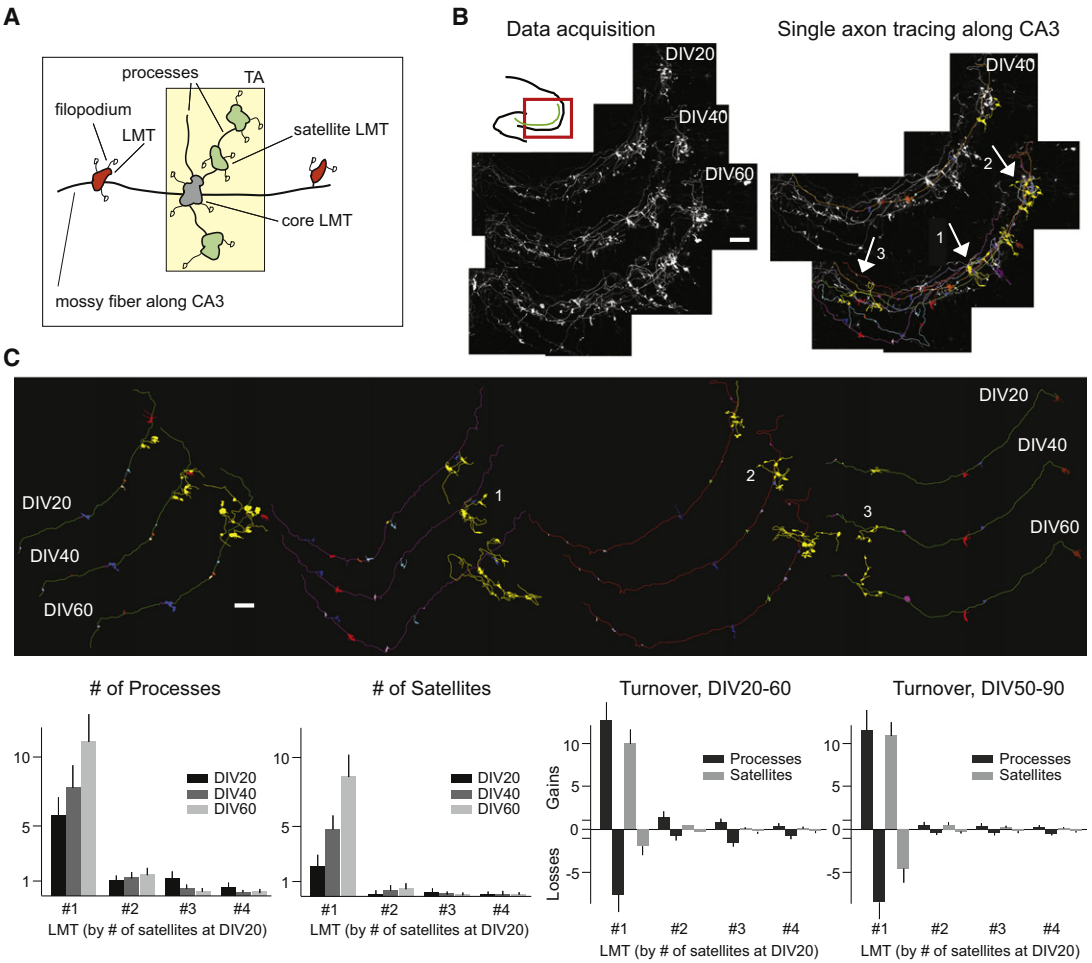

Figure 1. Si1-Mossy Fibers Exhibit 1 Distinct TA in Organotypic Slice Cultures

(A) Schematic of the terms used in this study for LMTs. Filopodia synapse onto inhibitory interneurons and are found at all types of LMTs. Processes are longer than filopodia (>20 μm). TAs consist of a core LMT, of processes, and of satellite LMTs. (B) Illustration of single mossy fiber tracing procedure. Complete stacks were acquired and tiled for the same slice cultures at DIV20, 40, and 60. In the camera lucidas, individual axons and their terminals are in different colors. LMTs with satellites and processes (i.e., TAs) are always yellow. Three TAs are indicated by the arrows and numbers, and shown again in (C). (C) Analysis of LMT dynamics at individual mossy fibers. For quantitative analysis, LMTs of individual mossy fibers were reordered according to decreasing numbers of satellite and processes at DIV20. n = 30 mossy fibers, from five independent slice cultures. Bars: 100 μm.

can cause an expansion of the terminal-rich area by the mossy fiber projection in CA3 (Pleskacheva et al., 2000; Ramírez-Amaya et al., 2001; Magariños et al., 2006), and environmental enrichment can augment the birth, survival, and maturation of adult-born GCs (van Praag et al., 2000). At the level of individual terminals in CA3, structural remodeling involves the turnover of dynamic synapses with inhibitory interneurons, and the turnover of satellite LMTs (Figure 1A) (De Paola et al., 2003; Galimberti et al., 2006). In adult mice, this remodeling can produce sustained alterations of connectivity, including an increase in the frequency of satellite LMTs when mice are housed under enriched environment (EE) conditions, and a gradual life-long shift in the distributions of LMT sizes, from a homogeneous distribution in young mice to one consisting of many very small LMTs and a few extremely large LMTs in old mice (Galimberti et al., 2006; Gogolla et al., 2009). The characteristic arrangement, consisting of a core LMT and satellite LMTs connected to each other through processes, identifies some LMT complexes as Terminal Arborizations (TAs; Figure 1A). Such TAs are found in many types of axons, where they consist of a local axonal side-branch, which produces multiple local synapses through its secondary side-processes (Gogolla et al., 2007). Notably, TAs are particularly structurally plastic (De Paola et al., 2006), and can thus explore significant volumes of synaptic territory, but the mechanisms that set up and regulate these major sites of structural plasticity in the adult have remained unclear.

Studies of developmental synaptogenesis, and of synaptic plasticity in vitro, have uncovered molecular mechanisms that may have a role in defining sites of structural plasticity in the adult. Intercellular adhesion at the synapse promotes synaptogenesis and synaptic growth, but tends to prevent structural

plasticity. Structural plasticity studies have focused on the roles of the cell adhesion molecule NCAM and its posttranslational modification through polysialic acid (PSA), which negatively modulates adhesion and is well correlated with enhanced structural plasticity during development and in the adult (Seki and Rutishauser, 1998; Lopez-Fernandez et al., 2007; Rutishauser, 2008; Bisaz et al., 2009; Bonfanti and Theodosis, 2009). Structural plasticity is further coupled to functional modifications of synapses through the trafficking and accumulation of postsynaptic receptor subunits (e.g., the AMPA receptor subunit GluR1) and the assembly of postsynaptic scaffolds (Kopec et al., 2007; De Roo et al., 2008b; Nikonenko et al., 2008; Kessels and Malinow, 2009). Interestingly, signaling molecules involved in guiding axons have also been implicated in synaptogenesis and synaptic plasticity, providing attractive potential mechanisms to couple plasticity to positional information within target regions. These studies have focused in particular on the possible roles of Eph/ephrin signaling pathways in regulating synaptic growth and maintenance (Grunwald et al., 2004; Lim et al., 2008; Klein, 2009). Taken together, the results of these mechanistic studies provide attractive candidate mechanisms to control and pattern structural plasticity, but the roles of any of these mechanisms in setting up structurally plastic synapses in the adult have not been explored.

Here we investigated how structural plasticity is set up in individual mossy fibers in CA3. We show that 30%–35% of hippocampal mossy fibers, exemplified by the reporter transgenic line *Thy1-mGFP*^{si1} (Lsi1 mice), exhibit one distinct TA, whereas 10%–15% of mossy fibers (e.g., line *Thy1-mGFP*^{si2} [Lsi2 mice]) exhibit >2 distinct TAs. The remaining mossy fibers exhibit no detectable TAs. These defined TAs account for most structural plasticity by LMTs in CA3. We show that TAs are specified in juvenile mice through a process leading to the retention of high densities of synaptic sites specifically at core LMTs of TAs. Unexpectedly, mossy fibers establish their single or most vigorous TAs at a position along CA3 that is topographically related to the position of the GC along the DG. In juvenile circuits, but not more mature circuits, enzymatic removal of PSA from NCAM leads to the establishment of >2 TAs in single-TA mossy fibers, but does not abolish a topographic preference for those TAs. By contrast, specifically interfering with EphA4 activation not only leads to the formation of >2 TAs in single-TA mossy fibers, but also disrupts the topographic specification of TAs. These results suggest the existence of TA specification processes based on GC identity in juvenile animals, which define spatially restricted structural plasticity sites in the adult. Surprisingly, the results further suggest that connectivity, and thus possibly information processing in the hippocampus, involves topographic principles.

RESULTS

Individual Mossy Fibers Exhibit Distinct Terminal Arborizations

To determine whether LMTs belonging to the same hippocampal mossy fiber may differ in the extent to which they exhibit structural plasticity, we carried out time-lapse imaging experiments in organotypic slice cultures derived from Lsi1 reporter mice, which overexpress membrane-targeted GFP (mGFP) in few DG GCs (De Paola et al., 2003; Gogolla et al., 2006). We imaged the same cultures at 20 day intervals, starting from day in vitro (DIV) 20. In order to allow a complete analysis of mossy fibers projecting along the entire extent of CA3, we acquired high-resolution images including the entire thickness of the slices throughout CA3. Individual images were then tiled, and stacks of data were analyzed three-dimensionally, in order to resolve and trace individual axons and all their LMTs in CA3 (Figure 1B; see Figure 1A for definitions of LMT structures analyzed in this study).

We found a dramatic focalization of all process outgrowth and satellite LMTs to 1 TA per mossy fiber (Figures 1B and 1C). A comparable concentration of structural remodeling to 1 TA was detected in 57/60 mossy fibers, from 10 independent slice cultures; the remaining 3/60 mossy fibers exhibited no LMT with at least one satellite throughout all imaging sessions. When comparing different mossy fibers, it became clear that highly plastic TAs could be detected at most positions along the proximo-distal axis of CA3 (Figures 1B and 1C). We generated structural plasticity values for individual LMT complexes by adding up large-scale remodeling events per core LMT (i.e. the LMT closest to the main axon, from which satellites stem; Figure 1A) between individual imaging sessions; these included the numbers of new or lost satellite LMTs (>3 μm diameter), and the numbers of new or lost processes (>10 μm) (Figure 1A). The analysis included all mossy fibers that could be traced unambiguously throughout CA3. For each individual mossy fiber, LMT complexes were then reordered based on decreasing structural plasticity, thus generating "structural plasticity profiles" for individual axons. An analysis of 60 such profiles revealed a highly significant concentration of most structural plasticity to 1 TA per mossy fiber in these slice cultures (Figure 1C). Notably, structural remodeling was restricted to the same TA through all imaging sessions, and in slice cultures of ages ranging from DIV20 to DIV150 (Figure 1C).

To determine whether individual mossy fibers also exhibit distinct TAs in vivo, we traced individual labeled axons in fixed preparations derived from 3-month-old Lsi1 mice. Although processes and satellites associated with LMTs were less prominent in these young mice than in the slice cultures, they were again restricted to 1 TA per axon (Figure 2A). We have reported that the occurrence of processes and satellite LMTs in CA3 stratum lucidum is greatly increased upon housing of mice under EE conditions (Galimberti et al., 2006; Gogolla et al., 2009). Tracing of individual axons from such EE mice now revealed that 1 TA per mossy fiber along CA3 expressed the vast majority of this experience-driven increase in LMT complexities upon EE (Figure 2B). We have further shown that the distribution of LMT sizes in CA3 stratum lucidum shifts gradually from a comparatively uniform distribution in young adult mice to a segregation into a majority of small LMTs and a minority of very large LMTs in old mice (Galimberti et al., 2006; Gogolla et al., 2009). Tracing of individual mossy fibers from mice of different ages now revealed a gradual increase in the numbers of processes and satellites by 1 TA per axon with increasing age (Figure 2C). This increased complexity was particularly dramatic in mice older than 18 months, where essentially all larger LMTs were

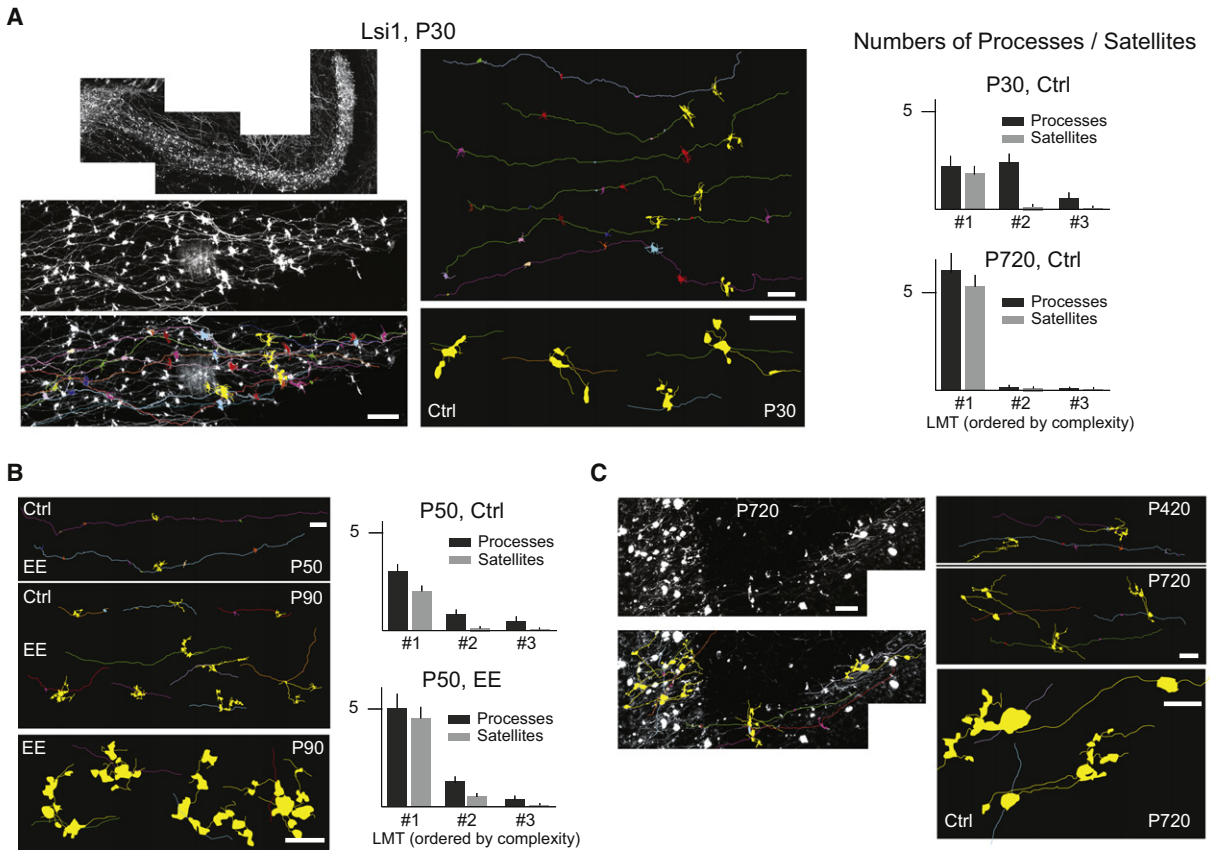

Figure 2. Si1-Mossy Fibers Exhibit 1 Distinct TA In Vivo

(A) (Left) Tracing of individual mossy fibers and their LMTs in a P30 Lsi1 mouse. In the camera lucidas, LMTs with satellites are indicated in yellow; the lower panel shows higher magnification examples of TAs. (Right) Quantitative analysis of LMTs with processes and satellites; reordering of LMTs as described in Figure 1C; n = 30 mossy fibers, from three mice each.

(B) (Left) Tracing of individual mossy fibers in P50 and P90 Lsi1 mice upon control or EE conditions. (Right) Quantitative analysis of the data; n = 30 mossy fibers, from three mice.

(C) Tracing of individual mossy fibers in 14-month-old and 24-month-old Lsi1 mice. The camera lucida on the lower right shows higher magnification examples of TAs at 24 months.

Bars: 25 μm.

either basal or satellite LMTs belonging to the same 1 TA per axon (Figure 2C). The analysis of fixed hippocampal preparations from Lsi1 mice of different ages, or housed under EE conditions, thus provided evidence that when LMT complexities or sizes increase in vivo, these changes are restricted to 1 TA per mossy fiber. Although repeated in vivo imaging of the same mossy fibers in the hippocampus was not possible for technical reasons, these results are consistent with the notion that, like in organotypic slice cultures, mGFP-positive mossy fibers of Lsi1 mice exhibit 1 distinct TA in CA3.

Subpopulations of Mossy Fibers with 0, 1, or >2 TAs

To determine whether all hippocampal mossy fibers exhibit 1 TA in CA3, we transfected DG GCs of wild-type mice with an mGFP expression construct in organotypic slice cultures (gene-gun transfection) or in vivo (low-titer lentivirus transduction; Dittgen et al., 2004), and analyzed labeled mossy fiber projections. Among the mossy fibers that we were able to trace in CA3, about 35% exhibited 1 TA with processes and satellites, 10%–15% of the mossy fibers exhibited >2 TAs with satellites and processes, and the remaining ca. 50% exhibited no satellites or long processes (Figure 3A; n = 30, from three mice each).

To investigate the possibility that there might be distinct subpopulations of mossy fibers differing in their numbers of TAs, we analyzed a second line of transgenic mice (Lsi2 mice) expressing mGFP in few hippocampal GCs. Labeled mossy fibers from Lsi2 organotypic slice cultures consistently exhibited >2 distinct TAs (Figure 3B). Out of 60 mGFP-positive Lsi2-mossy fibers (12 slice cultures), 1/60 exhibited 1 TA, 57/60 exhibited at least 2 TAs (42/60 at least 3 TAs), and 2/60 exhibited no TAs at DIV60. Importantly, the same TAs again maintained this distinction throughout our imaging experiments (Figure 3B). A comparison to Lsi1 slice cultures revealed that the additional TAs in the Lsi2 cultures were accompanied by a reduction in the extent of remodeling at the most plastic of the TAs (Figure 3B). The analysis of fixed hippocampal preparations from Lsi2 mice revealed

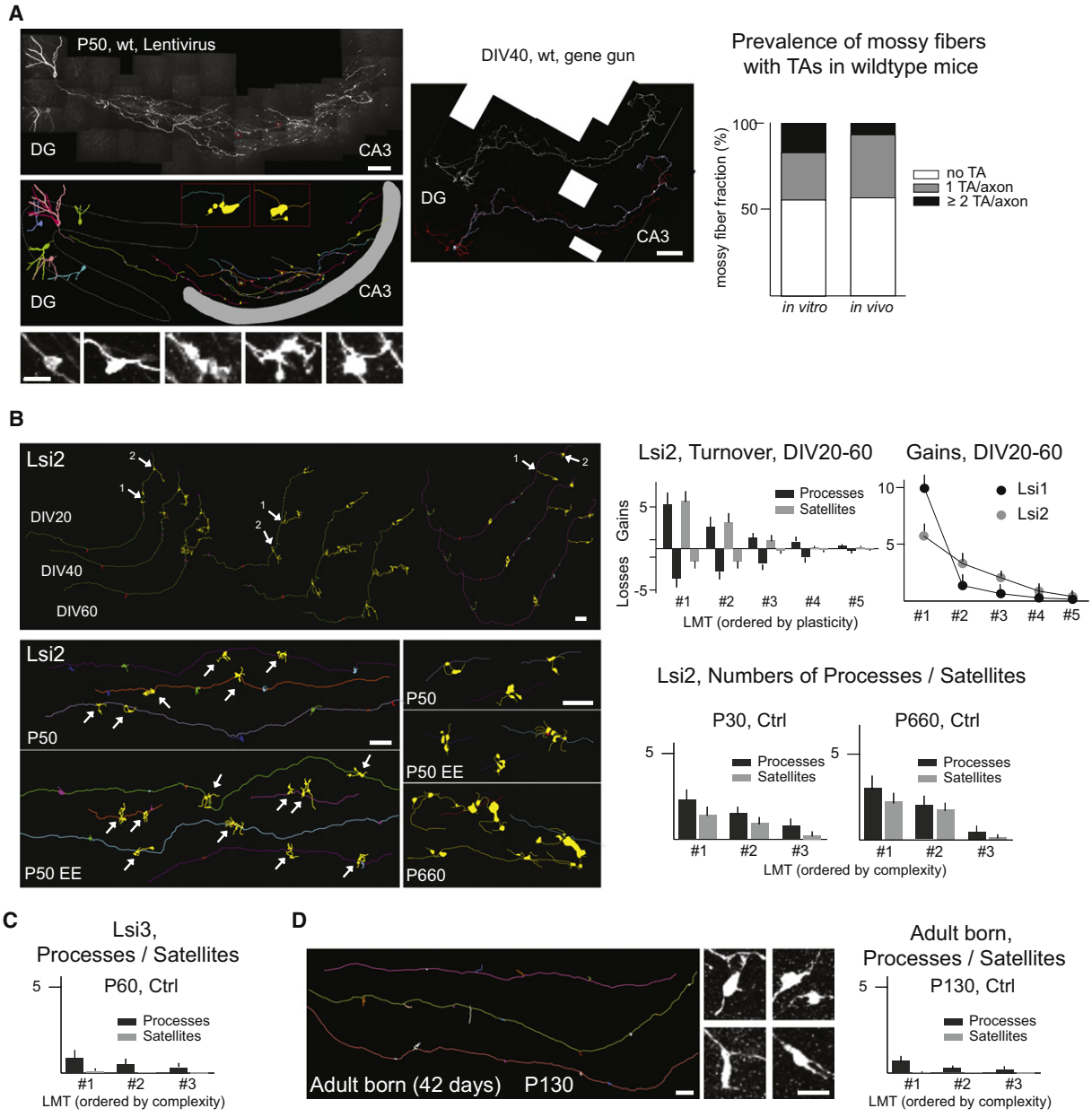

Figure 3. Hippocampal GCs with 1, >2, and 0 TAs along CA3

(A) Determination of TA frequencies in mossy fibers of nontransgenic mice. (Left) Lentiviral expression of mGFP in GCs in vivo, and tracing of labeled mossy fibers in CA3. Middle panel: camera lucidas of some of the mossy fibers shown in the upper panels; lower panel: individual LMTs without (two from left) or with satellites. (Center) mGFP labeling of GCs upon gene gun transfection in slices. (Right) Prevalence of mossy fibers with 0, 1, and >2 TAs in vivo and in slice cultures. n = 60 mossy fibers, from three mice each. The >2 TA group in vivo is underestimated due to the difficulty of tracing labeled mossy fibers throughout CA3.

(B) mGFP-positive mossy fibers in the reporter line Lsi2 exhibit >2 TAs. Camera lucidas and quantitative analysis are as described in Figures 1 and 2. Note vicinity of TA#1 and TA#2 in the lucidas from slice cultures (numbers) and in vivo (arrows). Also note how in comparison to Lsi1-mossy fibers, Lsi2-mossy fibers exhibit less remodeling (e.g., gains) at TA#1, and shallower remodeling gradients among their terminals. n = 30 mossy fibers from five independent cultures, or three mice each.

(C) Absence of mossy fiber terminals with satellites (i.e., TAs) in Lsi3-mossy fibers. n = 30 mossy fibers, from three mice.

(D) Absence of mossy fiber terminals with satellites (i.e., TAs) in adult-born GC mossy fibers. New GCs were virus labeled (Experimental Procedures) 6 weeks before the analysis. Small panels: examples of mGFP-labeled LMTs. n = 30 mossy fibers, from three mice.

Bars: 100 μm (A and B); 25 μm (D); 5 μm (A, D, and smaller panels).

the consistent presence of >2 distinct LMT complexes with processes and satellites per labeled mossy fiber under control and EE housing conditions in this second line of transgenic mice (Figure 3B).

A substantial fraction of randomly labeled mossy fibers exhibited no TAs in vivo and in vitro (Figure 3A), suggesting that additional subpopulations of GCs may not exhibit this form of structural plasticity. Indeed, labeled mossy fibers in a third transgenic line (*Thy1-mGFP*^{Lsi3}) exhibited no prominent TA (Figure 3C), and so did adult-born GCs (Figure 3D; see also Experimental Procedures). Taken together, these results suggest the existence of subpopulations of hippocampal GCs in the mouse exhibiting 0, 1, or >2 TAs per mossy fiber along CA3. For simplicity, we will designate mGFP-positive mossy fibers from Lsi1 and Lsi2 mice as Si1- and Si2-mossy fibers, respectively. Si1-mossy fibers thus exhibit one TA, whereas Si2-mossy fibers exhibit >2 TAs in CA3.

Core LMTs of TAs Exhibit Higher Synapse Densities

What might distinguish TAs from the other LMTs of a mossy fiber along CA3? Since the growth of axonal arborizations during development and the expansion of spines during plasticity have been related to the local strength of synapses (Meyer and Smith, 2006; Cline and Haas, 2008), we explored the possibility that what distinguishes TAs may also be correlated to synaptogenesis processes. We compared the densities of synaptic sites at LMTs belonging to the same mossy fiber. Previous detailed studies have shown how most synaptic sites inside the (mGFP-positive) outer boundaries of these giant terminals (Gogolla et al., 2006; Rollenhagen et al., 2007) can be assigned unambiguously to individual LMTs by immunocytochemistry (Gogolla et al., 2009), and how only a minority of synaptic sites (<10%) is located at the edge of those LMTs that are directly adjacent to an LMT from a different axon, thus precluding their unambiguous assignment. Antibodies against the presynaptic active zone protein Bassoon (tom Dieck et al., 1998) and the glutamatergic postsynaptic markers PSD95 and Pi-GluR1 (pGluR1) highlighted closely codistributed puncta at mGFP-positive LMTs in hippocampal stratum lucidum in vivo, and in organotypic slice cultures (Figure 4A). The numbers of these puncta corresponded closely to numbers of synapses determined from electron micrographs of stratum lucidum LMTs, and can therefore be considered as bona fide measures of synapse densities at these large presynaptic terminals (Gogolla et al., 2009). A quantitative analysis on fixed hippocampal preparations from 3-month-old Lsi1 mice revealed that core LMTs of putative TAs (defined as terminals with at least one satellite LMT) exhibited synapse densities that were on average 2.1-fold higher than any of the other LMTs by the same mossy fibers, including satellite LMTs (Figure 4B). Higher synapse densities (>1.5x of average) were detected at 19/20 core LMTs of putative TAs, but only at 3/100 LMTs without satellites, and at 0/30 satellite LMTs (Figure 4B). Synapse densities at LMTs were generally higher upon EE (Gogolla et al., 2009), but core LMTs of TAs continued to be the subpopulation with highest average densities under conditions of enhanced plasticity (not shown). The TAs of Si2-mossy fibers also exhibited higher synapse densities at their core LMT (Figure 4B), suggesting that the higher numbers of TAs did not reflect the loss of a distinction over non-TA LMTs, but rather the specification of more TAs in Si2-mossy fibers.

To investigate how higher synapse densities at core LMTs may relate to the emergence of TAs in maturing hippocampal circuits, we analyzed Si1-mossy fibers in organotypic slice cultures. Synapse density values in the slice cultures were comparable to those detected in vivo (Figure 4C). Like their counterparts in vivo, core LMTs belonging to TAs of Si1-mossy fibers exhibited synapse densities that were substantially higher than those of all the other LMTs (Figure 4C). Notably, at DIV8 when first processes and satellite LMTs became detectable, synapse densities were undistinguishable among all the LMTs of mossy fibers, and exhibited high values comparable to those of core LMTs of TAs in more mature mossy fibers (Figure 4C). Over the following 6–10 DIV, mossy fiber maturation involved a general expansion in volume, but a reduction in synapse densities at all LMTs, except for core LMTs of TAs (Figure 4C). Taken together, these results suggest that the emergence of TAs in maturing circuits is correlated with the maintenance of higher synapse densities, specifically at core LMTs of TAs (Figure 4D). These higher synapse densities at core LMTs are then maintained for at least 5 months in organotypic slice cultures, and possibly throughout life in vivo. The results further suggest that differences in TA numbers between Si1- and Si2-mossy fibers reflect the specification of 1 TA in Si1-mossy fibers, but of >2 TAs in Si2-mossy fibers.

Topographic Distribution of TAs along CA3

What might be the functional logic underlying the specification of 1 or a few individual TAs in Si1- and Si2-mossy fibers? Given the fact that pyramidal neurons with cell bodies at different positions along the proximo-distal axis in CA3 differ systematically in the spread of their recurrent collaterals within CA3 and in the positions of their axonal terminations in CA1 (Ishizuka et al., 1990), we wondered whether single TAs are specified at random positions along CA3, or whether specification may reflect some anatomical principle. We therefore traced Si1-mossy fibers from organotypic slice cultures all the way back to the corresponding GCs in the DG (Figure 5A), and determined whether the positions of their cell bodies exhibit any relationship to the position of their TAs. The analysis revealed the existence of a striking colinear topographic relationship: GCs at the outer end of the upper DG blade established TAs at the most distal end of CA3, GCs at the crest of the DG established TAs about halfway along CA3, and GCs at the outer end of the lower blade established TAs most proximally in CA3 (Figure 5B). To exclude the possibility that this topographic relationship might be peculiar to Si1-mossy fibers or to Lsi1 mice, we transfected mGFP into slice cultures from nontransgenic mice using a gene gun procedure, and analyzed mossy fibers with TAs. When the positions of GCs in the DG, and the most prominent TA along CA3, were plotted for individual mossy fibers, Si1 and gene gun data fitted readily into the same relationship (Figure 5B; combined slope: $r = 0.77$; probability that linear regressions for Lsi1 and gene gun data differ: $p = 0.38$). To investigate whether TAs in Si2-mossy fibers are also specified at preferred positions, we determined how frequently TA#2 (i.e., the second-most vigorous TA) was a direct neighbor of TA#1. We found that in most cases,

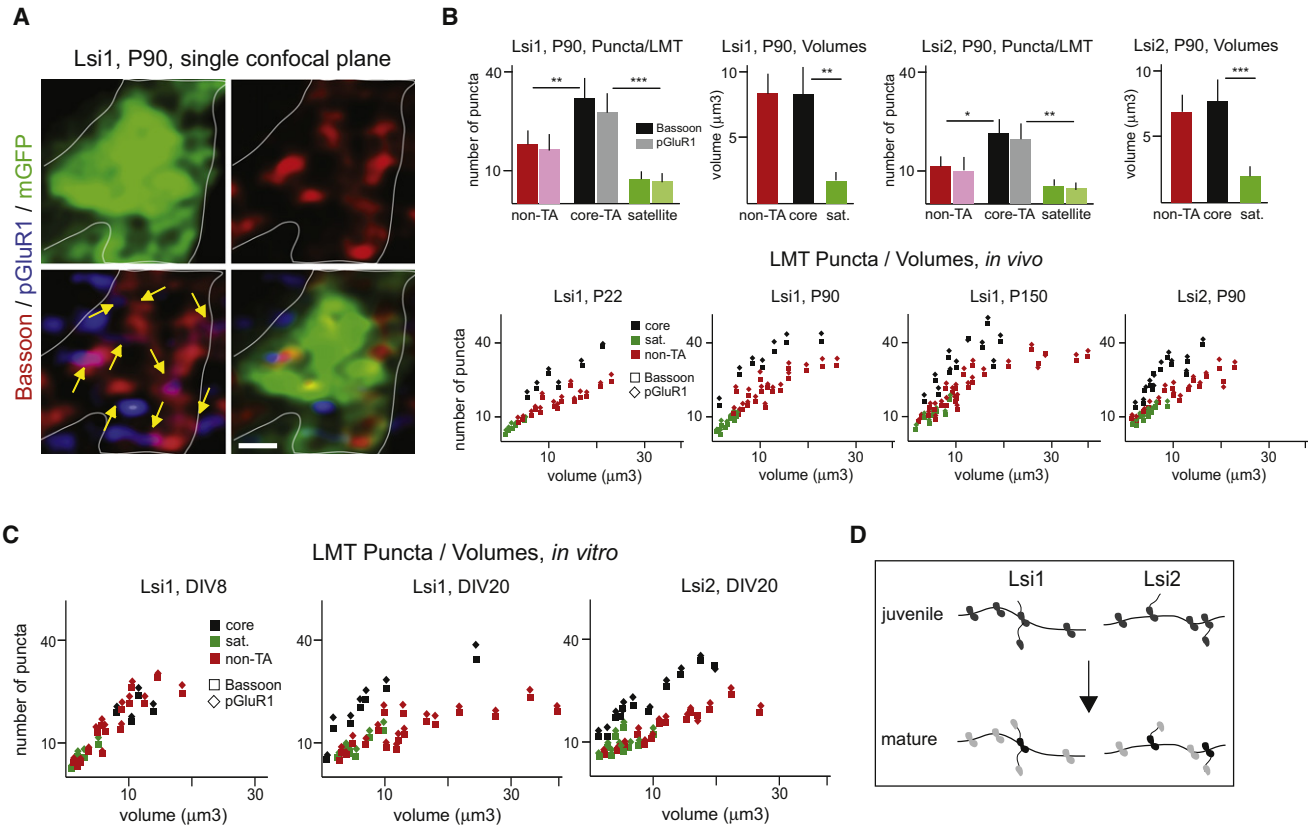

Figure 4. Core LMTs of TAs Exhibit Higher Densities of Synaptic Puncta

(A) High-magnification view of LMTs in Si1-mossy fibers counterstained for Bassoon and Pi-GluR1 (pGluR1). Note close correspondence between Bassoon and pGluR1 puncta (arrows); outline of LMT is highlighted by white line. Due to the nonsaturating settings and the single confocal plane analysis, the mGFP signal in the images does not consistently match the outlines of the LMT (see Results and Experimental Procedures).

(B) Higher densities of synaptic puncta at core LMTs of TAs in vivo. Upper graphs: average numbers of Bassoon (darker) and pGluR1 (lighter) puncta per LMT, and average LMT volumes for non-TAs (red), core LMTs (black), and satellite LMTs (green) in P90 Lsi1 and Lsi2 mice. Student t test; *$p < 0.01$, **$p < 0.001$, ***$p < 0.0001$. Lower graphs: scatter plots of LMT volumes versus Bassoon and pGluR1 puncta. Note how core LMTs of TAs consistently exhibit higher puncta densities, irrespective of age or genotype.

(C) Selective retention of higher synaptic puncta densities at core LMTs of TAs in maturing slice cultures. Note how all LMTs exhibit high puncta densities at DIV8, but only core LMTs retain them at DIV20 in Lsi1 and Lsi2.

(D) Schematic of how core LMTs of TAs retain higher synaptic puncta densities irrespective of GC subtype. Dark color: higher synaptic puncta densities. Bar: 1 µm.

TA#2 was either a next neighbor or in close vicinity of TA#1 (Figure 5C).

We then determined whether TAs also form at topographically predetermined positions along CA3 in vivo. Except for rare exceptions with very low numbers of transgene-expressing cells, we were not able to trace back Si1-mossy fibers to their GC of origin due to the high density of collaterals in the hilus region of the DG. Instead, we carried out lentivirus transduction experiments, where we targeted mGFP expression to GCs within a subregion of the DG in vivo. We found that the position of transduced GCs was predictive of the position of LMTs with satellites and processes, and that the relationship between GC position in the DG and TA position along CA3 was closely comparable in vivo and in slice cultures (Figure 5D). Due to the comparatively high numbers of labeled GCs in these experiments, we could not discriminate between mossy fibers with 1 or several TAs. The results thus further support the notion that mossy fibers with >1 TA also place their most plastic TAs at topographically preferred positions. In further support of this notion, and similarly to the analysis of TAs in slice cultures, we found that TA#2 was in most cases a close neighbor of TA#1 in Lsi2 mice (Figure 5E). We conclude that for GCs with TAs, there is a colinear topographic relationship between the position of the GCs in the DG and the position of their TAs in CA3.

Specification of TAs in Juveniles Influenced by PSA

To investigate the mechanisms underlying TA specification in hippocampal mossy fibers, we determined whether their properties and topography might depend on the presence of NCAM, a broadly expressed cell adhesion molecule that has been involved in synaptic plasticity, and that accounts for most linked PSA at the surface of neurons, i.e., a major determinant of structural plasticity in the nervous system (Seki and Rutishauser, 1998; Cremer et al., 1998; Rutishauser, 2008; Bisaz et al., 2009).

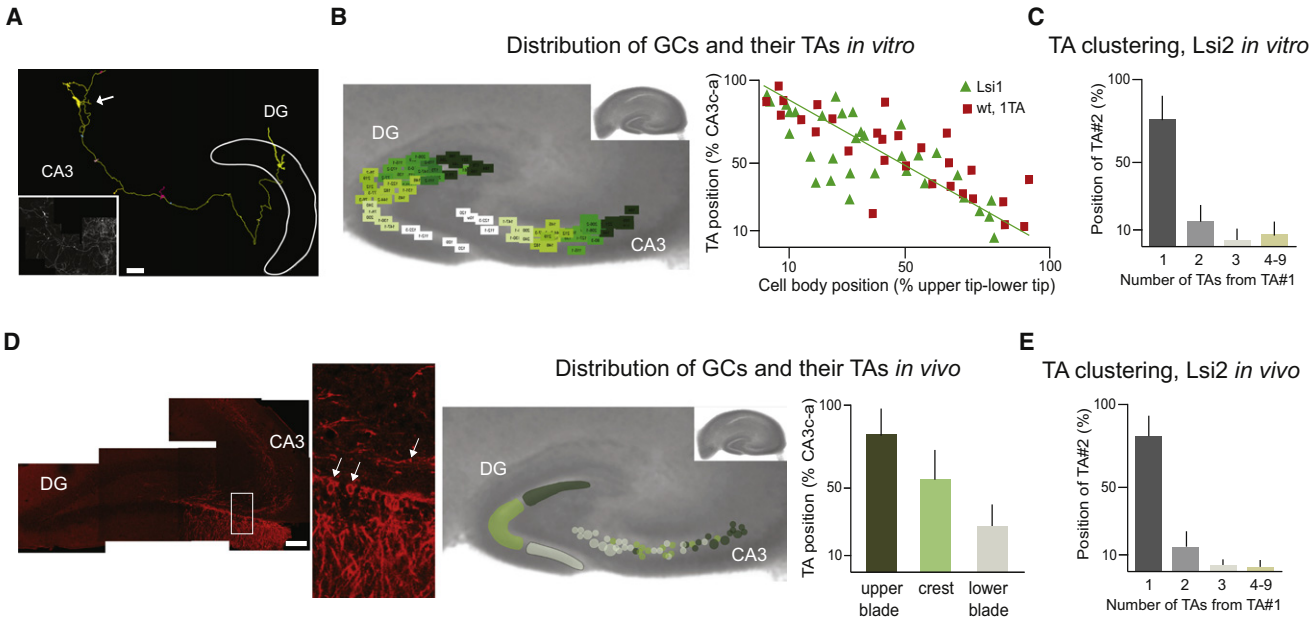

Figure 5. Topographic Distribution of TAs

(A) Camera lucida and mGFP fluorescence image (inset) of gene gun experiment to trace the position of individual GCs and their TAs (arrow). DG outline: based on NeuN staining.

(B) Topographic distribution of TAs in slice cultures. (Left) Results for individual GCs superimposed onto a hippocampus slice. The color code was defined by the position of individual TAs (numbers); corresponding GC cell bodies were then assigned the same code. (Right) Scatter plot of the results. Red squares: gene gun data (wild-type mice; mossy fibers with 1 TA); green triangles: Lsi1 data (green line: trend line). The 0%/0% point on the graph corresponds to a GC position at the tip of the upper blade, and a TA at the proximal end of CA3c.

(C) Spatial proximity of TA#1 and TA#2 in Si2-mossy fibers in vitro. A value of 1 means that TA#2 is a direct neighbor of TA#1. n = 30 mossy fibers, from eight slice cultures.

(D) Topographic distribution of TAs in vivo. (Left) Example of virus application at distal end of lower DG blade; a magnified view of the inset is shown on the right panel (arrows: labeled GCs and LMT). (Center) Results for individual TAs superimposed onto a hippocampal slice. GC positions are defined as broad domains of virus-driven expression, and in turn define the color code for TAs. The positions of individual TAs are plotted for the three types of injections; circle sizes reflect TA sizes at that position. The experiment does not discriminate between mossy fibers with 1 or several TAs. (Right) Quantitative analysis; n = 40, from two mice each (5.5 months).

(E) Spatial proximity of TA#1 and TA#2 in Si2-mossy fibers in vivo. n = 30 mossy fibers, from three Lsi2 mice (P90).

Bar: 25 μm (A); 100 μm (C).

We crossed Lsi1 and Lsi2 mice into an *NCAM*$^{-/-}$ background (Cremer et al., 1994) and analyzed Si1- and Si2-mossy fiber terminals along CA3. In the absence of NCAM, Si1-mossy fibers, which consistently exhibit 1 TA in a wild-type background, exhibited multiple TAs in organotypic slice cultures and in vivo (Figures 6A and 6B). Notably, the excess of Si1-mossy fiber TAs in the absence of NCAM was accompanied by a reduction in the extent of structural remodeling at the most plastic TA, and in a markedly reduced remodeling gradient between the individual LMTs of Lsi1-mossy fibers (Figure 6B). The excess Lsi1 TAs maintained this distinction for at least 4 months in the slice cultures, and exhibited elevated synaptic puncta densities at their core LMTs, suggesting that the increase in the number of TAs by Si1-mossy fibers in the absence of NCAM did not reflect a loss in the distinction between TAs and the other LMTs along the same mossy fiber (Figure S1, available online). As in Lsi2-mossy fibers, the positions of TA#1 and TA#2 were closely correlated in Si1-mossy fibers in the absence of NCAM (Figure S1).

The analysis of randomly labeled mossy fibers revealed a major increase in the fraction of mossy fibers with multiple TAs in the absence of NCAM (Figure 6B). However, nearly half of the randomly labeled mossy fibers continued to lack TAs in the absence of NCAM, suggesting that subpopulations of GCs do not exhibit this form of structural plasticity irrespective of the presence or absence of NCAM (Figure 6B). Notably, the position of the most plastic TAs (TA#1) in Si1 and in randomly labeled mossy fibers continued to exhibit topographic preference (Figure 6B), suggesting that the absence of NCAM interferes with the concentration of structural plasticity onto a single TA in Si1-mossy fibers, but does not suppress their topographic bias with respect to position along CA3.

To explore the possibility that PSA on NCAM might account for the number of TAs along Si1-mossy fibers, we first determined whether and when PSA could be detected along these mossy fibers. In young (DIV8) organotypic slice cultures from Lsi1 mice, Si1-mossy fibers clearly exhibited PSA immunoreactivity (Figure 6C). As expected, cultures from mice lacking NCAM exhibited no detectable PSA signal (not shown). In good correspondence with the intensities of stratum lucidum PSA profiles in vivo, PSA signals along mossy fibers had decreased at

DIV20, and were weak at DIV30 (Figure 6C). Treatment of the slice cultures with endoneuraminidase-N (endoN), an enzyme that specifically cleaves linked PSA from NCAM, led to a major reduction of the PSA signal in the organotypic slice cultures (Figure 6C). Continuous treatment with endoN from DIV8 on led to the appearance of >2 TAs per Si1-mossy fiber, and in randomly labeled mossy fibers in the slices (Figure 6D). Again, the endoN treatment did not suppress a topographic bias for the most plastic TAs (Figures 6D and S1). Therefore, the acute removal of PSA in wild-type hippocampal slice cultures is sufficient to mimick an *NCAM*$^{-/-}$ background with respect to the numbers of TAs formed by hippocampal mossy fibers.

The accumulation of PSA on NCAM has been associated with enhanced plasticity during critical periods in mammalian nervous system development (Di Cristo et al., 2007; Rutishauser, 2008). Accordingly, we determined whether TAs on hippocampal mossy fibers might be sensitive to PSA removal during a critical period postnatally. Removal of PSA between DIV4 and DIV8 or between DIV8 and DIV12 produced an increase in the numbers of TAs per mossy fiber that was comparable to that achieved with a continuous endoN treatment throughout the culture time (Figure 6D). As in slice cultures lacking NCAM, the excess of TAs was accompanied by reduced remodeling at the most plastic TA, and a reduced plasticity gradient along Si1-mossy fibers (Figure 6D). Si2-mossy fibers also exhibited a reduced plasticity gradient upon removal of PSA (Figure S1). The extra Si1 TAs induced in the slice cultures by a treatment with endoN between DIV8 and DIV12 exhibited comparable elevated synapse densities at their core LMTs, and the position of TA#2 was closely correlated to that of TA#1 (Figure S1). In stark contrast, when applied after DIV20 endoN did not detectably affect TAs along Si1-mossy fibers (Figure 6D). These results suggested that TAs along hippocampal mossy fibers are specified during a sensitive period in juveniles, through a mechanism influenced by the presence of PSA on NCAM. PSA influenced the numbers of TAs and plasticity differences among TAs, but not TA specification per se, nor their topographic distributions.

Topographic Specification of TAs Involves EphA4 Signaling

To further investigate what might underlie the relationship between the position of GCs within the DG and the position of their TAs along CA3, we analyzed the transcriptomes of GCs and CA3 pyramidal neurons for the presence of gradients of known guidance molecules and their receptors. Narrow transversal stripes of DG or CA3 principal neuron layers were collected from frozen sections of P10 dorsal hippocampus using a laser dissection microscope (Figure 7A). RNA was then submitted to two rounds of amplification, and probes were hybridized to mouse Affimetrix gene chips (Saxena et al., 2009). We found that several candidate guidance molecules were expressed in gradients along CA3, including the ephrins A3 and B2, the Eph-Receptors A3, A5, A7, A10, and B1, the semaphorins 3D, 5A, and 6D, and the Slit-like family members 1 and 4 (Figure 7B; Table S1, available online). By contrast, among ephrin and semaphorin ligands and receptors, EphA4 mRNA was the only species consistently exhibiting a gradient along the DG (Figure 7B; Table S1). In situ hybridization and immunocytochemistry experiments confirmed the presence of transcript and protein gradients in dorsal hippocampus at P10, i.e., at the postnatal time likely to be relevant for TA specification (Figure 7C).

To investigate the possibility that EphA4 might be critically involved in the topographic distribution of mossy fiber TAs, we carried out interference experiments in organotypic slice cultures using reagents that have been shown to interfere with the activation of EphA4 or of ephrins signaling to EphA4 (Murai et al., 2003a, 2003b). A KYLPYWPVLSSL (KYL) peptide (see Experimental Procedures for full sequence) known to suppress EphA4 activation consistently produced >2 TAs in Si1-mossy fibers (Figure 8A, B). By contrast, a WASHAPYWPHPP (WAS) peptide that inhibits EphA7, but not EphA4, did not detectably affect TA distributions (Figures 8A and 8B). Excess TAs in the presence of KYL peptide consistently exhibited higher densities of synapses at their core LMTs (Figure 8B). Application of the KYL peptide to young slice cultures (DIV0–10) was sufficient to increase TA numbers in Si1-mossy fibers (Figure 8B). In parallel, the peptide produced reduced remodeling at the most plastic TA and shallow plasticity gradients along Si1 mossy fibers (Figure 8B). The peptide was still effective when treatments were started at DIV10, but was ineffective when applied after DIV20 (Figure 8B). An EphA4-Fc chimera, which sequesters ephrins that signal to EphA4, had an effect closely comparable to the KYL peptide (Figures 8C and 8E). The KYL peptide did not cause TA formation in Si3-mossy fibers, suggesting that it specifically affects TA specification patterns in mossy fibers competent to form TAs (Figure 8D). In further support of this notion, the KYL peptide produced >2 TAs in about half, but not all, randomly labeled mossy fibers (Figure 8E). Finally, and most notably, the KYL peptide and the EphA4-Fc chimera abolished the topographic arrangement of TAs along CA3 (Figure 8F). The KYL peptide also abolished the topographic arrangement of TAs in endoN-treated slices (not shown). Taken together, these results provide evidence that interfering with EphA4 function during a sensitive period postnatally is sufficient to disrupt topographic patterns of TA specification in mossy fibers.

DISCUSSION

We have investigated the mechanisms underlying the specification of stable and structurally plastic synaptic terminals in the adult, using hippocampal mossy fibers and their TAs as a model system. We provide evidence that TAs with high plasticity properties are specified during a sensitive period in juvenile circuits, and that they maintain that distinction in the adult, leading to a focusing of structural plasticity at defined positions along CA3. Subpopulations of GCs exhibit 0, 1, or >2 TAs along their mossy fibers. Notably, mossy fibers with TAs establish these according to a topographic bias, in a process depending on EphA4 signaling during a sensitive period. In addition, disruption of EphA4 signaling or of PSA-NCAM in juvenile circuits led to the formation of >2 TAs by single-TA mossy fibers, suggesting the involvement of intra-axonal competition mechanisms in TA specification. We discuss possible implications of these findings, and their relationship to previous studies of synapse selection and structural plasticity in neuronal circuits.

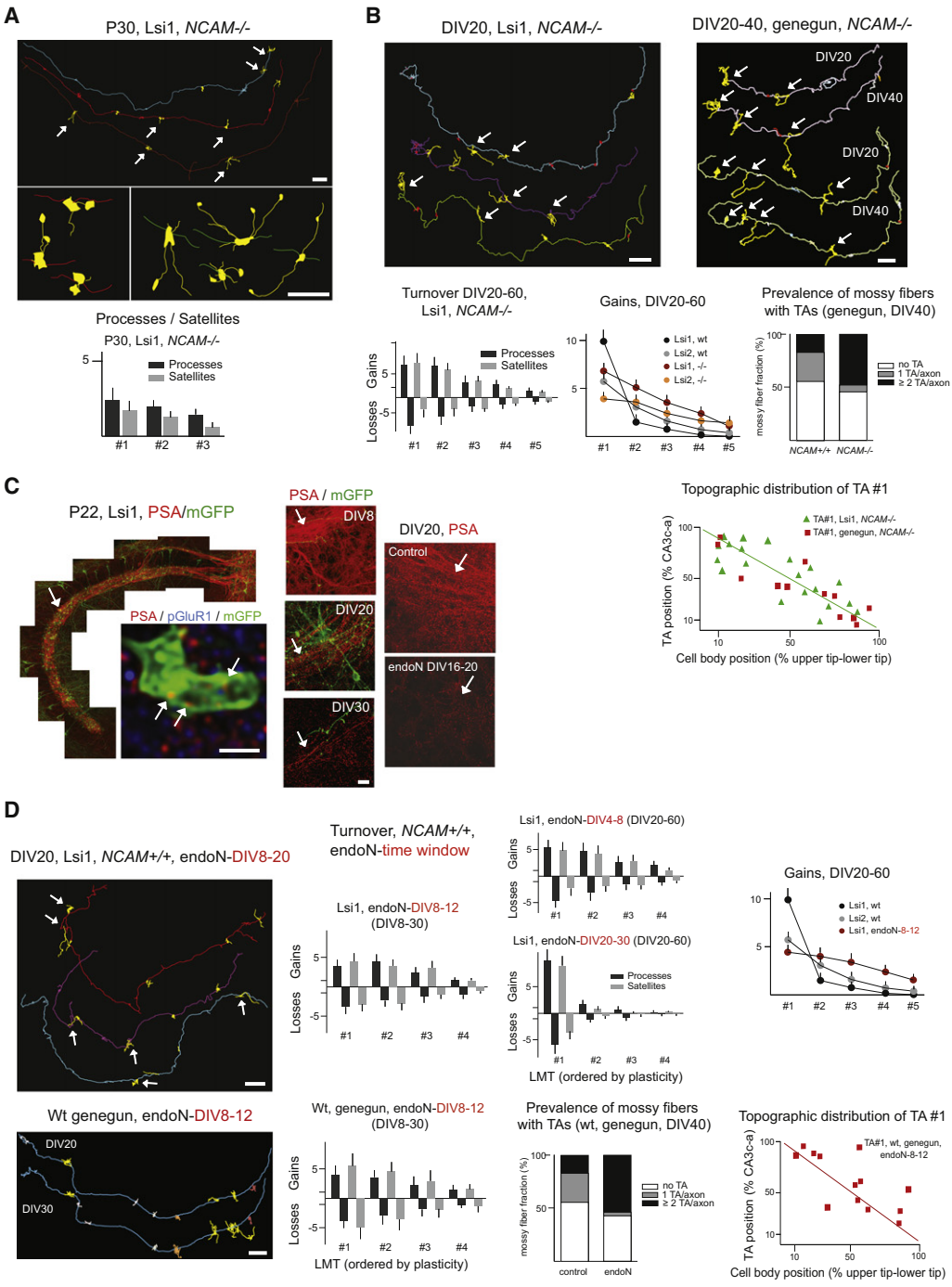

Figure 6. Specification of Single TAs in Juvenile Circuits Depending on PSA-NCAM

(A) In the absence of NCAM, Si1-mossy fibers exhibit >2 TAs in vivo. Camera lucidas and quantitative analysis are as described in Figure 3B. Lower panels: higher magnification views of TAs belonging to two distinct (red and green) mossy fibers.

(B) In the absence of NCAM, about half of mossy fibers, and nearly all Lsi1-mossy fibers, exhibit >2 TAs in slice cultures. Left, Si1-mossy fibers; right, gene gun labeled mossy fibers with TAs at DIV20 and DIV40. Camera lucidas and quantitative analysis are as described in Figures 1C, 3A, 3B, and 5B. Note how about half of randomly labeled mossy fibers continue to lack TAs in the absence of NCAM; also note how the most plastic TA (TA#1) continues to exhibit topographic preference in the absence of NCAM.

(C) Expression of PSA on juvenile mossy fibers, and removal with endoN. (Left) Low-magnification view of Si1-mossy fiber projection counterstained for PSA, and high-magnification view of individual LMT counterstained for PSA and pGluR1 (single confocal plane); arrows: individual PSA puncta. (Right) PSA signal at mossy fiber projection (arrows) in slice cultures from Lsi1 mice, and removal of PSA signal upon 4 day treatment with endoN. Note gradual decrease of PSA signal between DIV8 and DIV30.

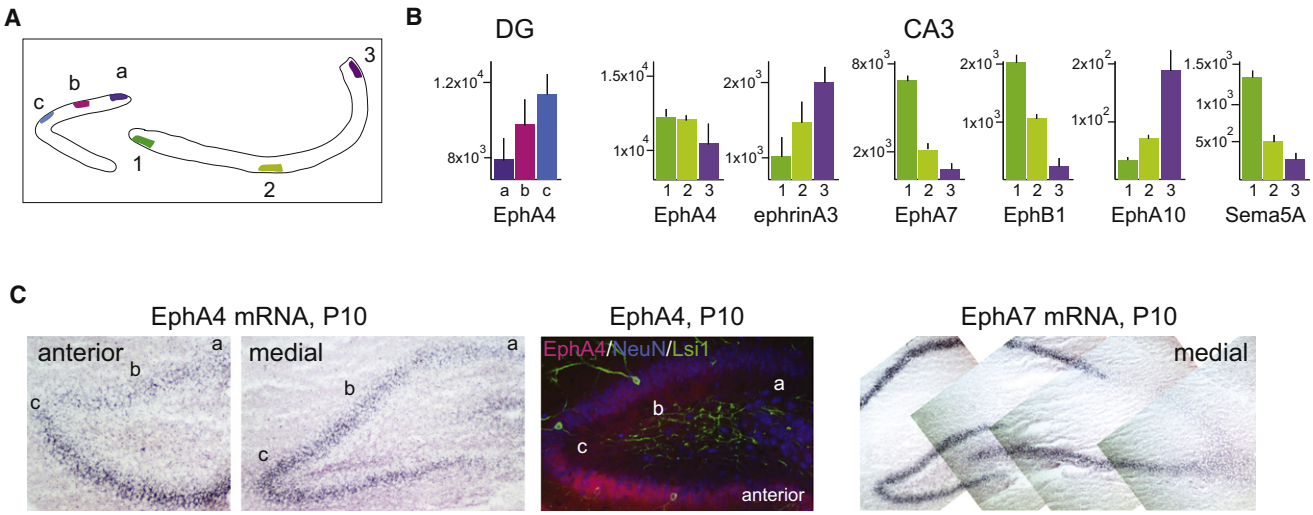

Figure 7. Guidance Molecule Transcripts Expressed in Gradients along the Juvenile DG or CA3

(A) Schematic of cell positions and their color code for the microarray analysis.

(B) Raw expression values for individual transcripts at P10. Averages and standard errors are from three mice each.

(C) In situ hybridization (EphA4 and EphA7) and immunocytochemistry (EphA4; Lsi1 mouse) in P10 hippocampus. Letters (a, b, c) indicate DG positions as in the schematic shown in (A). Note gradients for EphA4 along DG (highest at distal lower blade) and for EphA7 in CA3 (highest proximal CA3c), in agreement with microarray data.

See also Table S1.

GC Subpopulations with 0, 1, and >2 TAs

Our analysis of randomly labeled mossy fibers has revealed that 50%–55% of all GCs exhibit no LMTs with detectable satellites (i.e., no TAs), and that among the GCs with TAs, 60%–70% of them have a single TA, whereas the others exhibit >2 TAs. Notably, mGFP-positive mossy fibers from Lsi1 and Lsi2 mice consistently exhibited 1 and >2 TAs, respectively, in slice cultures and in vivo, suggesting that mossy fibers with 1 or >2 TAs reflect genetically distinct subpopulations of GCs. We have so far been unable to find experimental conditions leading to a persistent absence of prominent TAs along Si1- or Si2-mossy fibers in the presence of synaptic activity, suggesting that GCs may differ in some intrinsic manner with respect to whether or not they establish TAs along their mossy fibers in CA3. Consistent with this notion, reporter-expressing GCs in Lsi3 mice, and adult-born GCs, exhibited no noticeable TAs, suggesting that TA-free mossy fibers may also reflect genetically distinct GCs. Furthermore, when the specification of a single TA in juvenile Si1 or randomly labeled mossy fibers was perturbed in the absence of PSA-NCAM or EphA4 signaling, Si1 and most randomly labeled mossy fibers exhibited >2 TAs, but these treatments did not alter the fraction of randomly labeled mossy fibers without TAs. Taken together, these results suggest that GCs can be subdivided into those that do or do not establish TAs along their mossy fibers in CA3, that GCs with TAs can establish by default >2 of them, and that GCs with a single TA restrict TA formation to one prominent one, in a process depending on PSA-NCAM and EphA4 signaling.

The observation that subpopulations of GCs can exhibit 0, 1, or >2 TAs is reminiscent of recent reports that axons of different types of neurons can establish many, few, or even no TAs within the same brain structure (e.g., neocortex; Portera-Cailliau et al., 2005; De Paola et al., 2006). Our results extend those previous observations by showing that in hippocampal mossy fibers the presence of TAs reflects local specification events, which take place in juvenile circuits, and which reflect genetically defined intrinsic properties of presynaptic neurons. Taking advantage of the unique anatomical properties of mossy fibers along CA3, our results further reveal a remarkable degree of specificity among the GC subpopulations with TAs. Thus, single TAs seem to be specified through a "winner-takes-all" mechanism, and according to an unsuspected topographic principle. A topographic principle also governs TA specification in GCs with >2 TAs, and no additional TAs appear to form after the specification period in juveniles, suggesting that, here too, patterns set up in juveniles predetermine sites of structural plasticity in the adult.

Mechanisms Underlying the Specification and Maintenance of TAs

We provide evidence that while "regular" and satellite LMTs exhibit comparable synaptic puncta per volume, core LMTs of TAs consistently exhibit 1.5- to 2-fold higher densities of

(D) EndoN treatment in juvenile cultures allows formation of >2 TAs in Si1-mossy fibers, and in a majority of randomly labeled mossy fibers. Camera lucida and quantitative analysis are as described in Figures 1C, 3A, 3B, and 5B. Note how endoN induces >2 TAs when applied at DIV4–8 or DIV8–12, but not from DIV20 on. Only mossy fibers with TAs were included in the turnover and topographic analysis of gene gun labeled cultures.

Bars: 25 μm (A, B, C [right], D); 1 μm (C, left). See also Figure S1.

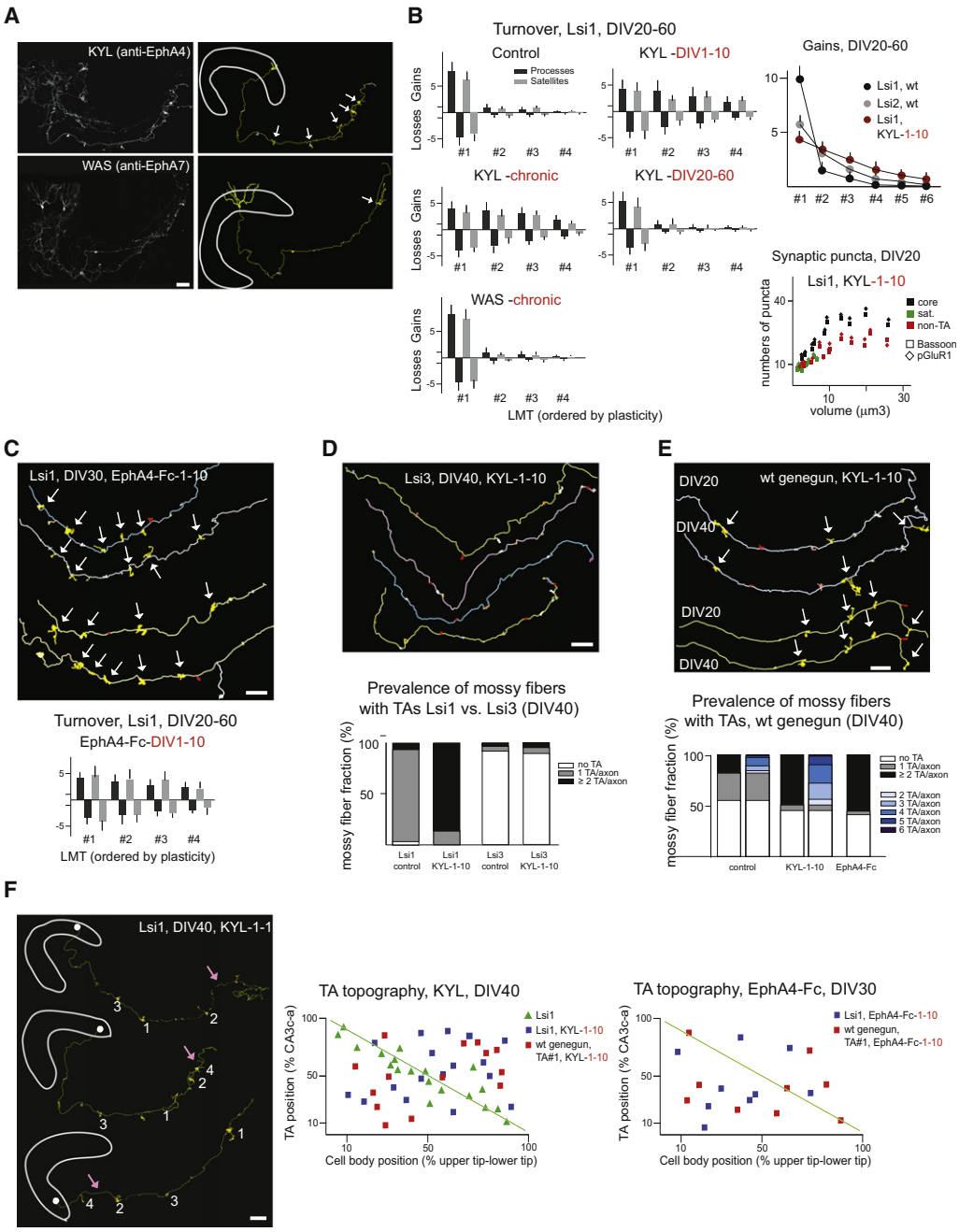

Figure 8. Topographic TA Specification Depends on EphA4 Signaling in Juvenile Hippocampal Circuits

(A) DIV30 slices from Lsi1 mice treated chronically with inhibitory KYL (EphA4) or WAS (EphA7) peptide. (Right) Camera lucida tracings of a representative GC with its TAs (arrows).

(B) Analysis of satellite and filopodia turnover in peptide-treated Lsi1 slices. Details are as described in Figures 1C, 3B, and 4C. n = 20 mossy fibers each, from five independent slice cultures.

(C) TA numbers and plasticity in EphA4-Fc treated Lsi1 slices.

(D) EphA4 inhibition does not induce TA formation in Lsi3-mossy fibers. Details as in Figure 3A.

(E) EphA4 inhibition in randomly labeled mossy fibers. Lucidas: tracings of randomly labeled mossy fibers with TAs in slices treated with KYL peptide. Details are as in Figure 3A.

(F) Inhibiting EphA4 signaling disrupts TA topography. (Left) Camera lucida tracings of Lsi1-mossy fibers and cell body positions. 1–4: TAs #1–4; pink arrows: approximate position of TA#1 as would be predicted from cell body position. Quantitative analysis is as in Figure 5B.

Bars: 25 μm. See also Figure S2.

synaptic puncta in organotypic slice cultures and in vivo. This observation strongly suggests that core LMTs, and therefore TAs, reflect a distinct specification mechanism. This distinction was detected for all TAs analyzed in our study, in slice cultures, or in vivo, and irrespective of whether they had been specified under control conditions or upon perturbation of PSA-NCAM or EphA4 signaling. Therefore, higher synaptic puncta densities at core LMTs are a defining feature of hippocampal mossy fiber TAs. In further support of this notion, differences in synaptic puncta densities among LMTs became apparent within the time window at which TA specification can be influenced by PSA or EphA4 signaling. Interestingly, all LMTs exhibited high synaptic puncta densities at DIV8, but only core LMTs of TAs retained this distinction at DIV20. This observation is in line with evidence discussed below suggesting that the initial selection of particular LMTs is followed by conditions preventing TA specification at the other LMTs of the same mossy fiber. These results relating the density of synaptic puncta to TA specification raise the intriguing possibility that TA specification and the striking structural plasticity at TAs may be coupled to synaptic strength during the maturation of hippocampal circuits. Such a coupling would be reminiscent of how synaptogenesis and the strengthening of developing synapses is coupled to the growth of terminal arbors within a target region (Meyer and Smith, 2006; Cline and Haas, 2008). However, whether the specification of TAs at hippocampal mossy fibers exhibits mechanistic similarities to ''synaptotrophic'' mechanisms of terminal arbor growth remains to be determined. Likewise, while there may be mechanistic resemblances in how ephrin/Eph signaling selects terminal arbors in developing optic tectum and TAs at maturing mossy fibers (O'Leary and McLaughlin, 2005), probing the extent to which this may reflect mechanistic similarities will require additional studies.

Our study provides evidence that TAs are specified during a sensitive period in juvenile circuits, through mechanisms involving the retention of synaptic complexes at core LMTs of TAs. While our study does not address the mechanisms that ensure the perpetuation of structural plasticity at those original TAs, our results do provide some insights into the mechanisms involved in the initial specification of TAs. PSA-NCAM has been implicated in structural plasticity through the negative modulation of adhesive interactions that favor stability and thus prevent structural remodeling (Rutishauser, 2008). Alternative modes of action of PSA, e.g., involving neurotrophin recruitment, also predict enhanced synaptic plasticity through PSA-NCAM. A plasticity-enhancing role for the PSA moiety on NCAM is consistent with the results of studies on axon guidance and synapse remodeling during sensitive periods in juvenile circuits, including the mossy fiber system, and upon behavioral protocols enhancing structural plasticity in the adult (Seki and Rutishauser, 1998; Hanson and Landmesser, 2004; Lopez-Fernandez et al., 2007; Rutishauser, 2008; Bisaz et al., 2009). Our findings may reflect a general reduction in synapse stabilization by mossy fiber PSA-NCAM, which may enhance the threshold for core LMT selection and thus TA formation during circuit maturation. In a similar manner, opposite gradients of EphA4 in GCs and of its ligands in pyramidal neurons along CA3 (e.g., ephrinA3, which exhibits a gradient consistent with a role in the topographic specification of TAs) may specify regions of minimal relative repulsion for individual mossy fibers (Lim et al., 2008; Klein, 2009; Tremblay et al., 2009). These may promote topographic TA specification, e.g., through interaxonal competition mechanisms. In the absence of PSA-NCAM, EphA4 signaling would continue to bias the selection of TAs within preferred regions along CA3, whereas in the absence of EphA4 signaling, reduced repulsion would now allow selection throughout a wider range of positions along CA3. Our results further suggest that the initial preferential selection of core LMTs may counteract TA formation at other positions along the mossy fiber. This might for example involve the selective sequestration of synaptogenic molecules and/or a protection against synapse-destabilizing mechanisms at the nascent core LMT. In the absence of PSA or of EphA4 signaling, more core LMTs and TAs can form along a mossy fiber, but these may have a smaller relative advantage in sequestering synaptogenic components, leading to weaker structural plasticity and shallower plasticity gradients among the TAs of a mossy fiber. Such mechanisms of synapse selection and intra-axonal competition (Fitzsimonds and Poo, 1998) are highly reminiscent of winner-takes-all mechanisms that have been proposed to account for the elimination of supernumerary axons at neuromuscular junctions (Kasthuri and Lichtman, 2005), and for competition among neighboring and distant synapses in circuit assembly and synaptic plasticity (Govindarajan et al., 2006; Harvey and Svoboda, 2007; De Roo et al., 2008b).

What might distinguish mossy fibers with 0, 1, and >2 TAs? mGFP-positive mossy fibers and LMTs in Lsi1 mice did not exhibit noticeably higher PSA-NCAM signals than their Lsi2 counterparts (not shown), arguing against the possibility that Lsi1-mossy fibers would be subject to extra repulsive regulation favoring the establishment of 1 TA per mossy fiber. Likewise, we did not detect any obvious difference in the labeling intensity or numbers of PSA puncta at core or noncore LMTs of Lsi1- or Lsi2-mossy fibers (not shown), arguing against the possibility that local difference in PSA-NCAM may underlie TA specification. No obvious differences in EphA4 in situ hybridization signals were detectable among neighboring GCs within the same inner-outer layers of the DG, but we cannot exclude the possibility that slightly lower EphA4 signaling in Lsi2-mossy fibers may underlie the specification of several TAs in these mossy fibers. Likewise, comparable EphA4 in situ hybridization signals among neighboring GCs would argue against the possibility that Lsi3-mossy fibers lack prominent TAs due to higher EphA4 signaling. Mossy fibers with no TAs may express lower levels of critical components favoring synaptic growth and/or process outgrowth during circuit maturation. Consistent with this possibility, Si3-mossy fiber LMTs (and adult-born mossy fiber LMTs) were smaller and less heterogeneous in shape than their Si1 and Si2 counterparts. By contrast, mossy fibers with 1 TA may be more sensitive to local regulation of synaptic growth than those with >2 TAs. In support of this possibility, Si1 LMTs were generally larger than Si2 LMTs. More in-depth studies involving local perturbation strategies in Lsi1 and Lsi2 slice cultures should provide further insights into how synaptogenesis mechanisms may be coupled to the specification of 1 or several TAs in mossy fibers.

Positional differences along the proximo-distal axis in CA3 have been reported in previous studies (Ishizuka et al., 1990),

and our observations that several molecules implicated in axon guidance exhibit expression gradients in CA3 are consistent with those previous reports. By contrast, no topographic organization had been reported along the DG for any given septo-temporal position. We found no correlation between the times at which newborn GCs exit the cell cycle during development, and the position of their cell bodies along the DG blades (Figure S2), but some developmental maturation in the DG does proceed from the tip of the upper blade to the tip of the lower blade (Henze et al., 2000). The EphA4 mRNA gradient at P10 exhibited a similar orientation (lower in more mature cells; Figure 7C), and a decrease in DG EphA4 mRNA with maturation has been reported in a previous study (Tremblay et al., 2009). GCs may thus use transient developmental maturation gradients in EphA4 levels to select the position of their TAs along CA3. However, we did not detect obvious signs of maturational gradients for LMTs along the distal-proximal axis of CA3 (Figure S2), suggesting that the establishment of topographic patterns by TAs may not be coupled directly to the sequence of maturation of GCs along DG blades.

Implications for Information Processing in the Adult Hippocampus

Our results have revealed an unsuspected level of spatial organization in hippocampal circuits. Thus, our findings provide evidence that for mossy fibers exhibiting prominent structural plasticity, most of this plasticity is persistently focused to one or a few positions along CA3, and that the positions of the most vigorous TAs are defined according to a topographic rule. Given that experience and age have pronounced effects on the complexities of TAs (Galimberti et al., 2006; Gogolla et al., 2009), our results suggest that the selection of particular positions along CA3 by TAs might have functional significance for information flow in the hippocampus. It seems further likely that satellites from TAs at any position along CA3 will locally compete with LMTs from different mossy fibers for postsynaptic space on pyramidal neuron dendrites. Accordingly, our findings suggest that the growth and remodeling by individual TAs will be associated with redistribution processes of synaptic inputs onto individual pyramidal neurons within that region of CA3. For mossy fibers with several TAs, the relative plasticity of each TA may be altered as a consequence of such redistribution processes, providing further potential substrates for experience-dependent structural plasticity in the adult. Within such a potentially dynamic context, the processes that lead to the specification of particular TAs at particular positions along CA3 in juvenile circuits acquire further potential significance for adult plasticity.

Exploring the functional implications of our findings will require physiology- and behavior-based approaches well beyond the scope of the current study. However, what is currently known about hippocampal anatomy, and about the spatial organization of information flow in entorhinal cortex, is consistent with the notion of spatially organized processing in hippocampal circuits. Thus, pyramidal neurons at different positions along CA3 differ dramatically in the target regions of their axonal projections within CA3 and to CA1 (Ishizuka et al., 1990). In contrast to CA3, no topographic organizational principles had been described before in the DG. Our finding that the position of GCs predicts the position of their TAs in CA3 thus raises the intriguing possibility that information flowing from the entorhinal cortex to CA3 via the DG may be organized according to anatomically defined principles (see also Dolorfo and Amaral, 1998; Fyhn et al., 2004).

EXPERIMENTAL PROCEDURES

Mice and Reagents

Transgenic mice expressing membrane-targeted GFP in small subsets of neurons (*Thy1-mGFP*^{Si1} [L21] and *Thy1-mGFP*^{Si2} [L15]) were as described (De Paola et al., 2003). NCAM knockout mice (Cremer et al., 1994) were generously provided by Harold Cremer (Marseille), and were backcrossed into *Thy1-mGFP* reporter mice. *Thy1-mGFP*^{Lsi3} mice were generated by by M. Sigrist and S. Arber (Basel).

EE procedures were as described (Gogolla et al., 2009). Organotypic slice cultures were based on the Stoppini method (Stoppini et al., 1991), as described (De Paola et al., 2003). Coordinates for lentiviral injections into mouse DG were (in mm from Bregma): −2.18 posterior, 1.5 side, 1.77 down (infrapyramidal blade); −2.18 posterior, 1.75 side, 1.65 down (suprapyramidal blade); −2.18 posterior, 0.8 side, 1.84 down (crest).

Antibodies were from the following sources: Bassoon, anti-mouse Alexa Fluor 546 and 647, anti-goat Alexa Fluor 546 and 633, goat-anti-mouse IgM Alexa Fluor 546, donkey anti-goat Alexa Fluor 568 (Molecular Probes); NeuN anti-mouse (Chemicon); pGluR1 (Sigma; 1:200); PSA-NCAM, clone 2-2B (Millipore, 1:500); EphA4 (sc-921, Santa Cruz; 1:25). EndoN was from Sigma (working concentration 0.1 U/ml). The peptides KYL and WAS were synthesized by Bachem (Bubendorf, Switzerland); peptide quality was verified by mass spectrometry and RP-HPLC; working concentrations were 2 μM (Murai et al., 2003a). EphA4-Fc (Murai et al., 2003b) was from Sigma (working concentration: 9 μg/ml, applied from DIV0 to DIV10). Lentiviral constructs were a generous gift from Pavel Osten (Cold Spring Harbor Laboratories; Dittgen et al., 2004); cytosolic GFP was replaced in the expression cassette by the mGFP sequence. Plasmids for gene gun transfection of hippocampal neurons were a kind gift from Thomas Oertner (FMI); the plasmids drive the expression of membrane-targeted tdRFP or GFP under the Synapsin1 promoter. A modified MML virus to drive the expression of Cre recombinase in dividing GCs was a kind gift from Fred Gage (Salk Institute) (Tashiro et al., 2006). The virus was injected into the DG of 3-month-old male mice carrying a loxP-STOP-loxP-mGFP construct under the control of the panneuronal promoter Tau (kind gift from Silvia Arber, FMI). Mice were analyzed for GFP signals 6 weeks postinjection. Adult-born GC labeling was verified in pilot experiments upon analysis at 1, 2, and 4 weeks postinjection. For BrdU analysis, mice were injected with two consecutive shots (24 hr apart) of a 10 mM filter-sterilized solution of BrdU (100 mM/kg) in PBS.

Immunocytochemistry, In Situ Hybridization, and Microarrays

Vibratome sections were of 60 μm thickness. Free-floating sections were then postfixed with 50% Ethanol in PBS for 15–20 min, and subsequently permeabilized/blocked for 3 hr at RT in 20% BSA/0.5% Triton X-100 in PBS. Sections were then incubated with primary, and subsequently secondary, antibody (3–4 hr at RT each in 5% BSA in PBS). BrdU detection was carried out in P30 mice that had been perfused with 4% PFA with 0.8% picric acid in PBS. Slices were incubated for 30 min in 1M HCl at 45°C, washed twice with PBS, neutralized in Borate buffer, and then stained with rat-antiBrdU (1:500 Abcam).

In situ hybridization was performed according to a standard protocol, using Digoxigenin-labeled probes for nonradioactive detection. The sequences of the specific probes against EphA4, EphA7, and ephrinA3 mRNA are provided in Supplemental Information. All samples belonging to the same series were processed in one batch, and images were acquired and processed with the same settings.

Gene profiling of identified mGFP-positive cells in CA3 and DG was as described (Saxena et al., 2009). Equivalents of 15–20 (CA3) and 30 (DG) were collected for three independent mice, for each sample. Present calls ranged between 44.5% and 50.1%.

Image Acquisition and Analysis

Male mice were perfused transcardially with 100 ml ice-chilled 4% paraformaldehyde in PBS; brains were collected and kept in fixation solution over-ight at 4°C. Vibratome coronal sections (100–150 μm) were cut the next day using a LEICA VT 100S vibratome (Leica) and mounted in Airvol for fluorescence imaging. For the analysis of mossy fiber projections in CA3, hippocampi were dissected and immersed separately in 35 mm culture dishes containing warm liquid 2% agarose in distilled water. Once agarose became solid, a cube containing the hippocampus was removed and placed onto a McIlwain Tissue Chopper. Ten to twelve sections transversal to the hippocampus long axis were collected and analyzed for fluorescence. High-resolution images were acquired on an upright spinning disc confocal microscope consisting of a Yokogawa CSU22 confocal scanning head mounted on a Zeiss Axioimager M1 using a 100x alphaPlan-Apochromat 1.45 (Zeiss) oil-immersion objective. Immunocytochemistry preparations were imaged on an LSM510 confocal microscope (Zeiss) using a 40x (1.4) oil-immersion objective. For lentiviral experiments in vivo, mice were analyzed 2 weeks after viral injection. For topography determinations, mice were injected with lentivirus at 5 months. Imaging of organotypic slice cultures was as described (Gogolla et al., 2006). Where indicated, drugs were replaced every 3–4 days, together with fresh medium. Biolistic transfections were carried out on DIV7–10 slice cultures using a Helios Gene Gun (BioRad).

Microscope images were processed and analyzed using Metamorph 6.1, Imaris 4.2 (Bitplane AG), and ImageJ software. We defined LMTs as mossy fiber terminal regions of >2.5 μm diameter in CA3a–c that were arranged either en-passant or as side structures connected to the mossy fiber axon or another LMT by an axonal process (satellite). For the quantification of LMT sizes in 3D (volumes), at least three confocal 3D stacks were acquired in CA3b for each preparation (three mice per condition) and analyzed using Imaris 4.2 software. Nonsaturating imaging conditions were chosen for all size analyses. An intensity threshold of 300 was chosen to selectively analyze LMTs (excluding axons and other smaller objects). All identified objects were verified by eye inspection. Generally, the settings for the analysis were identical for all samples of all ages, but in some cases we verified the settings through internal calibration using the diameters and signal intensities of axons. For the quantification of process/satellite turnover in slice cultures, individual mGFP-positive mossy fibers were traced in CA3 (but not the hilus) on a stitched image using Imaris 4.2 and a Wacom pen screen. Each mossy fiber was solved with all its LMTs, filopodia, processes, and satellite LMTs. For LMT or process turnover, gains or losses of satellite LMTs or processes between two imaging sessions were recorded; for each individual LMT or core LMT all gains or losses between DIV20–40 and between DIV40–60 were summed; in the plots, LMTs were arranged in decreasing order of satellite plus process numbers at DIV20. For the quantification of process/satellite numbers in vivo, individual mGFP mossy fibers were traced along CA3 (but not the hilus) similarly to those in slice cultures (>950 μm per mossy fiber, i.e., >85% along CA3).

For the quantitative analysis of Bassoon- and pGluR1-positive puncta per individual LMT, LMT volumes were first determined in 3D as described above. Confocal stacks were then opened individually, and for any given LMT, Bassoon and pGluR1 spots overlapping with the GFP signal (3D analysis) were counted on consecutive optical sections, throughout the entire z-extension of the terminal. Puncta that were continuous on consecutive sections were excluded (Gogolla et al., 2009).

SUPPLEMENTAL INFORMATION

Supplemental Information for this article includes two figures, one table, and Supplemental Experimental Procedures and can be found with this article online at doi:10.1016/j.neuron.2010.02.016.

ACKNOWLEDGMENTS

We are grateful to Patrick Schwarb, Aaron Ponti, and Jens Rietdorf for help with the imaging experiments; to Erik Cabuy for help with the identified cell genomics experiments; to Thomas Oertner for help with the gene gun transfection experiments; to Sarah Ruediger for the mGFP lentivirus construct; to Yuichi Deguchi for help with the in situ hybridization experiments; and to Markus Sigrist and Silvia Arber (FMI and Biozentrum, Basel) for generating and sharing Lsi3 transgenic mice. We thank Dominique Muller (CMU, University of Geneva), Jan Pielage (FMI, Basel), and Silvia Arber for valuable comments on the manuscript. This study is partially funded by the European Commission under the 7th Framework Programme (Collaborative Project Plasticise). The Friedrich Miescher Institut is part of the Novartis Research Foundation.

Accepted: January 31, 2010
Published: March 10, 2010

REFERENCES

Acsády, L., Kamondi, A., Sík, A., Freund, T., and Buzsáki, G. (1998). GABAergic cells are the major postsynaptic targets of mossy fibers in the rat hippocampus. J. Neurosci. *18*, 3386–3403.

Alvarez, V.A., and Sabatini, B.L. (2007). Anatomical and physiological plasticity of dendritic spines. Annu. Rev. Neurosci. *30*, 79–97.

Bisaz, R., Conboy, L., and Sandi, C. (2009). Learning under stress: a role for the neural cell adhesion molecule NCAM. Neurobiol. Learn. Mem. *91*, 333–342.

Bonfanti, L., and Theodosis, D.T. (2009). Polysialic acid and activity-dependent synapse remodeling. Cell Adh. Migr. *3*, 43–50.

Chklovskii, D.B., Mel, B.W., and Svoboda, K. (2004). Cortical rewiring and information storage. Nature *431*, 782–788.

Claiborne, B.J., Amaral, D.G., and Cowan, W.M. (1986). A light and electron microscopic analysis of the mossy fibers of the rat dentate gyrus. J. Comp. Neurol. *246*, 435–458.

Cline, H., and Haas, K. (2008). The regulation of dendritic arbor development and plasticity by glutamatergic synaptic input: a review of the synaptotrophic hypothesis. J. Physiol. *586*, 1509–1517.

Cremer, H., Lange, R., Christoph, A., Plomann, M., Vopper, G., Roes, J., Brown, R., Baldwin, S., Kraemer, P., Scheff, S., et al. (1994). Inactivation of the N-CAM gene in mice results in size reduction of the olfactory bulb and deficits in spatial learning. Nature *367*, 455–459.

Cremer, H., Chazal, G., Carleton, A., Goridis, C., Vincent, J.D., and Lledo, P.M. (1998). Long-term but not short-term plasticity at mossy fiber synapses is impaired in neural cell adhesion molecule-deficient mice. Proc. Natl. Acad. Sci. USA *95*, 13242–13247.

De Paola, V., Arber, S., and Caroni, P. (2003). AMPA receptors regulate dynamic equilibrium of presynaptic terminals in mature hippocampal networks. Nat. Neurosci. *6*, 491–500.

De Paola, V., Holtmaat, A., Knott, G., Song, S., Wilbrecht, L., Caroni, P., and Svoboda, K. (2006). Cell type-specific structural plasticity of axonal branches and boutons in the adult neocortex. Neuron *49*, 861–875.

De Roo, M., Klauser, P., Garcia, P.M., Poglia, L., and Muller, D. (2008a). Spine dynamics and synapse remodeling during LTP and memory processes. Prog. Brain Res. *169*, 199–207.

De Roo, M., Klauser, P., and Muller, D. (2008b). LTP promotes a selective long-term stabilization and clustering of dendritic spines. PLoS Biol. *6*, e219.

Di Cristo, G., Chattopadhyaya, B., Kuhlman, S.J., Fu, Y., Bélanger, M.C., Wu, C.Z., Rutishauser, U., Maffei, L., and Huang, Z.J. (2007). Activity-dependent PSA expression regulates inhibitory maturation and onset of critical period plasticity. Nat. Neurosci. *10*, 1569–1577.

Dittgen, T., Nimmerjahn, A., Komai, S., Licznerski, P., Waters, J., Margrie, T.W., Helmchen, F., Denk, W., Brecht, M., and Osten, P. (2004). Lentivirus-based genetic manipulations of cortical neurons and their optical and electrophysiological monitoring *in vivo*. Proc. Natl. Acad. Sci. USA *101*, 18206–18211.

Dolorfo, C.L., and Amaral, D.G. (1998). Entorhinal cortex of the rat: topographic organization of the cells of origin of the perforant path projection to the dentate gyrus. J. Comp. Neurol. *398*, 25–48.

Fitzsimonds, R.M., and Poo, M.M. (1998). Retrograde signaling in the development and modification of synapses. Physiol. Rev. *78*, 143–170.

Fyhn, M., Molden, S., Witter, M.P., Moser, E.I., and Moser, M.-B. (2004). Spatial representation in the entorhinal cortex. Science *305*, 1258–1264.

Galimberti, I., Gogolla, N., Alberi, S., Santos, A.F., Muller, D., and Caroni, P. (2006). Long-term rearrangements of hippocampal mossy fiber terminal connectivity in the adult regulated by experience. Neuron *50*, 749–763.

Gogolla, N., Galimberti, I., DePaola, V., and Caroni, P. (2006). Long-term live imaging of neuronal circuits in organotypic hippocampal slice cultures. Nat. Protoc. *1*, 1223–1226.

Gogolla, N., Galimberti, I., and Caroni, P. (2007). Structural plasticity of axon terminals in the adult. Curr. Opin. Neurobiol. *17*, 516–524.

Gogolla, N., Galimberti, I., Deguchi, Y., and Caroni, P. (2009). Wnt signaling mediates experience-related regulation of synapse numbers and mossy fiber connectivities in the adult hippocampus. Neuron *62*, 510–525.

Govindarajan, A., Kelleher, R.J., and Tonegawa, S. (2006). A clustered plasticity model of long-term memory engrams. Nat. Rev. Neurosci. *7*, 575–583.

Grunwald, I.C., Korte, M., Adelmann, G., Plueck, A., Kullander, K., Adams, R.H., Frotscher, M., Bonhoeffer, T., and Klein, R. (2004). Hippocampal plasticity requires postsynaptic ephrinBs. Nat. Neurosci. *7*, 33–40.

Hanson, M.G., and Landmesser, L.T. (2004). Normal patterns of spontaneous activity are required for correct motor axon guidance and the expression of specific guidance molecules. Neuron *43*, 687–701.

Harvey, C.D., and Svoboda, K. (2007). Locally dynamic synaptic learning rules in pyramidal neuron dendrites. Nature *450*, 1195–1200.

Henze, D.A., Urban, N.N., and Barrionuevo, G. (2000). The multifarious hippocampal mossy fiber pathway: a review. Neuroscience *98*, 407–427.

Henze, D.A., Wittner, L., and Buzsáki, G. (2002). Single granule cells reliably discharge targets in the hippocampal CA3 network in vivo. Nat. Neurosci. *5*, 790–795.

Holtmaat, A., Wilbrecht, L., Knott, G.W., Welker, E., and Svoboda, K. (2006). Experience-dependent and cell-type-specific spine growth in the neocortex. Nature *441*, 979–983.

Ishizuka, N., Weber, J., and Amaral, D.G. (1990). Organization of intrahippocampal projections originating from CA3 pyramidal cells in the rat. J. Comp. Neurol. *295*, 580–623.

Kasthuri, N., and Lichtman, J.W. (2005). The role of neuronal identity in synaptic competition. Nature *424*, 426–430.

Kessels, H.W., and Malinow, R. (2009). Synaptic AMPA receptor plasticity and behavior. Neuron *61*, 340–350.

Klein, R. (2009). Bidirectional modulation of synaptic functions by Eph/ephrin signaling. Nat. Neurosci. *12*, 15–20.

Kopec, C.D., Real, E., Kessels, H.W., and Malinow, R. (2007). GluR1 links structural and functional plasticity at excitatory synapses. J. Neurosci. *27*, 13706–13718.

Leutgeb, J.K., Leutgeb, S., Moser, M.B., and Moser, E.I. (2007). Pattern separation in the dentate gyrus and CA3 of the hippocampus. Science *315*, 961–966.

Lim, B.K., Matsuda, N., and Poo, M.M. (2008). Ephrin-B reverse signaling promotes structural and functional synaptic maturation in vivo. Nat. Neurosci. *11*, 160–169.

Lopez-Fernandez, M.A., Montaron, M.F., Varea, E., Rougon, G., Venro, C., Abrous, D.N., and Sandi, C. (2007). Upregulation of polysialylated neural cell adhesion molecule in the dorsal hippocampus after contextual fear conditioning is involved in long-term memory formation. J. Neurosci. *27*, 4552–4561.

Magariños, A.M., McEwen, B.S., Saboureau, M., and Pevet, P. (2006). Rapid and reversible changes in intrahippocampal connectivity during the course of hibernation in European hamsters. Proc. Natl. Acad. Sci. USA *103*, 18775–18780.

McBain, C.J. (2008). Differential mechanisms of transmission and plasticity at mossy fiber synapses. Prog. Brain Res. *169*, 225–240.

Meyer, M.P., and Smith, S.J. (2006). Evidence from in vivo imaging that synaptogenesis guides the growth and branching of axonal arbors by two distinct mechanisms. J. Neurosci. *26*, 3604–3614.

Mori, M., Abegg, M.H., Gähwiler, B.H., and Gerber, U. (2004). A frequency-dependent switch from inhibition to excitation in a hippocampal unitary circuit. Nature *431*, 453–456.

Murai, K.K., Nguyen, L.N., Koolpe, M., McLennan, R., Krull, C.E., and Pasquale, E.B. (2003a). Targeting the EphA4 receptor in the nervous system with biologically active peptides. Mol. Cell. Neurosci. *24*, 1000–1011.

Murai, K.K., Nguyen, L.N., Irie, F., Yamaguchi, Y., and Pasquale, E.B. (2003b). Control of hippocampal dendritic spine morphology through ephrin-A3/EphA4 signaling. Nat. Neurosci. *6*, 153–160.

Nikonenko, I., Boda, B., Steen, S., Knott, G., Welker, E., and Muller, D. (2008). PSD-95 promotes synaptogenesis and multiinnervated spine formation through nitric oxide signaling. J. Cell Biol. *183*, 1115–1127.

O'Leary, D.D., and McLaughlin, T. (2005). Mechanisms of retinotopic map development: Ephs, ephrins, and spontaneous correlated retinal activity. Prog. Brain Res. *147*, 43–65.

Pleskacheva, M.G., Wolfer, D.P., Kupriyanova, I.F., Nikolenko, D.L., Scheffrahn, H., Dell'Omo, G., and Lipp, H.P. (2000). Hippocampal mossy fibers and swimming navigation learning in two vole species occupying different habitats. Hippocampus *10*, 17–30.

Portera-Cailliau, C., Weimer, R.M., De Paola, V., Caroni, P., and Svoboda, K. (2005). Diverse modes of axon elaboration in the developing neocortex. PLoS Biol. *3*, e272.

Ramírez-Amaya, V., Balderas, I., Sandoval, J., Escobar, M.L., and Bermúdez-Rattoni, F. (2001). Spatial long-term memory is related to mossy fiber synaptogenesis. J. Neurosci. *21*, 7340–7348.

Rollenhagen, A., Sätzler, K., Rodríguez, E.P., Jonas, P., Frotscher, M., and Lübke, J.H. (2007). Structural determinants of transmission at large hippocampal mossy fiber synapses. J. Neurosci. *27*, 10434–10444.

Rutishauser, U. (2008). Polysialic acid in the plasticity of the developing and adult vertebrate nervous system. Nat. Rev. Neurosci. *9*, 26–35.

Saxena, S., Cabuy, E., and Caroni, P. (2009). A role for motoneuron subtype-selective ER stress in disease manifestations of FALS mice. Nat. Neurosci. *12*, 627–636.

Seki, T., and Rutishauser, U. (1998). Removal of polysialic acid-neural cell adhesion molecule induces aberrant mossy fiber innervation and ectopic synaptogenesis in the hippocampus. J. Neurosci. *18*, 3757–3766.

Stettler, D.D., Yamahachi, H., Li, W., Denk, W., and Gilbert, C.D. (2006). Axons and synaptic boutons are highly dynamic in adult visual cortex. Neuron *49*, 877–887.

Stoppini, L., Buchs, P.A., and Muller, D. (1991). A simple method for organotypic cultures of nervous tissue. J. Neurosci. Methods *37*, 173–182.

Tashiro, A., Zhao, C., and Gage, F.H. (2006). Retrovirus-mediated single-cell gene knockout technique in adult newborn neurons in vivo. Nat. Protoc. *1*, 3049–3055.

tom Dieck, S., Sanmartí-Vila, L., Langnaese, K., Richter, K., Kindler, S., Soyke, A., Wex, H., Smalla, K.H., Kämpf, U., Fränzer, J.T., et al. (1998). Bassoon, a novel zinc-finger CAG/glutamine-repeat protein selectively localized at the active zone of presynaptic nerve terminals. J. Cell Biol. *142*, 499–509.

Tremblay, M.E., Riad, M., Chierzi, S., Murai, K.K., Pasquale, E.B., and Doucet, G. (2009). Developmental course of EphA4 cellular and subcellular localization in the postnatal rat hippocampus. J. Comp. Neurol. *512*, 798–813.

van Praag, H., Kempermann, G., and Gage, F.H. (2000). Neural consequences of environmental enrichment. Nat. Rev. Neurosci. *1*, 191–198.